



Effect of gamma irradiation on X-ray absorption and photoelectron spectroscopy of Nd-doped phosphate glass

V. N. Rai,^{a,b,*} Parasmani Rajput,^c S. N. Jha,^c D. Bhattacharyya,^c
 B. N. Raja Shekhar,^c U. P. Deshpande^d and T. Shripathi^d

Received 9 June 2016

Accepted 9 September 2016

Edited by S. M. Heald, Argonne National Laboratory, USA

Keywords: glasses; XAFS; photoelectron spectroscopy; radiation damage; defect.

^aIndus Synchrotron Utilization Division, Raja Ramanna Centre for Advanced Technology, Indore 452013, India,

^bHomi Bhabha National Institute, Anushaktinagar, Mumbai-400094, India, ^cAtomic & Molecular Physics Division,

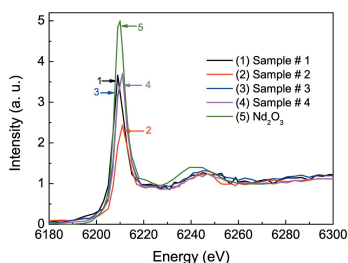
Bhabha Atomic Research Center, Trombay, Mumbai-400085, India, and ^dUGC-DAE Consortium for Scientific Research,

University Campus, Khandwa Road, Indore 452001, India. *Correspondence e-mail: vnrai@rrcat.gov.in

X-ray absorption near-edge structure (XANES) and X-ray photoelectron spectroscopy (XPS) of Nd-doped phosphate glasses have been studied before and after gamma irradiation. The intensity and the location of the white line peak of the L_3 -edge XANES of Nd are found to be dependent on the ratio O/Nd in the glass matrix. Gamma irradiation changes the elemental concentration of atoms in the glass matrix, which affects the peak intensity of the white line due to changes in the covalence of the chemical bonds with Nd atoms in the glass (structural changes). Sharpening of the Nd $3d_{5/2}$ peak profile in XPS spectra indicates a deficiency of oxygen in the glasses after gamma irradiation, which is supported by energy-dispersive X-ray spectroscopy measurements. The ratio of non-bridging oxygen to total oxygen in the glass after gamma radiation has been found to be correlated to the concentration of defects in the glass samples, which are responsible for its radiation resistance as well as for its coloration.

1. Introduction

The study of rare earth (RE) doped glasses and crystals has recently generated interest due to their importance in the development of many optoelectronic devices such as lasers, light converters, sensors, high-density memories, optical fibers and laser amplifiers (Gatterer *et al.*, 1998; Metwalli *et al.*, 2004; Karthikeyan & Mohan, 2004; Jayasankar *et al.*, 2008; Minami *et al.*, 1980; Jamnický *et al.*, 1995; Satyanarayana *et al.*, 1991; Seshadri *et al.*, 2010; Rai *et al.*, 2011; Kumar *et al.*, 2003; Sudhakar *et al.*, 2008; Dwivedi & Rai, 2012; Pérez-Rodríguez *et al.*, 2014). Various types of glasses, such as silicate, phosphate, borate, fluoride and telluride, have been used as the matrix for doping trivalent RE ions to produce various active optical devices such as lasers and infrared-to-visible up-conversion phosphors, *etc.* (Gatterer *et al.*, 1998; Metwalli *et al.*, 2004; Karthikeyan & Mohan, 2004; Jayasankar *et al.*, 2008; Minami *et al.*, 1980; Jamnický *et al.*, 1995; Satyanarayana *et al.*, 1991; Seshadri *et al.*, 2010; Rai *et al.*, 2011; Kumar *et al.*, 2003; Sudhakar *et al.*, 2008; Dwivedi & Rai, 2012; Pérez-Rodríguez *et al.*, 2014). In particular, RE doped glasses have been widely used as laser materials (Beber, 1986; Kumar *et al.*, 1997) because they can accommodate large concentrations of active ions without losing the useful properties of the material. These glasses are prepared with a certain range of compositional possibilities in order to facilitate tailoring of the physical, chemical and optical properties of interest for specific technological applications (Day *et al.*, 1998; Karabulut *et al.*, 2002; Balakrishnaiah *et al.*, 2006; Campbell & Suratwala, 2000;



Ajrout *et al.*, 2000; Hussin *et al.*, 2002). The radiative and non-radiative emission from such RE activated materials depends mainly on the local coordination environments and the spatial distribution of RE elements inside the host matrix. In this situation the characteristics of the chemical bonds formed by RE elements with their nearest neighbors also affect the optical properties of RE doped materials (Weber, 1990; Ebendorff-Heidepriem *et al.*, 1995).

Modifications of the optical and structural properties of glasses under the effect of high-energy radiation (UV, gamma rays and neutrons) have been of interest due to their wide application in optics on board space craft, in image guides for reactor inspection, in optical fiber guides as well as in mobilization of radioactive waste (Friebele, 1991; Rai *et al.*, 1986, 2010; Sharma *et al.*, 2006; ElBatal, 2007; Sandhu *et al.*, 2008; Sun *et al.*, 2008; ElBatal *et al.*, 2008, 2010; Abo-Naf *et al.*, 2008). Normally, structural changes in glasses after irradiation are found to be associated with the change in the concentration of atomic content in the glass matrix due to bond breaking and its possible reorganization, particularly the generation of different types of defects followed by the change in the color of the glasses (Friebele, 1991; Rai *et al.*, 1986, 2010; Sharma *et al.*, 2006; ElBatal, 2007; Sandhu *et al.*, 2008; Sun *et al.*, 2008; ElBatal *et al.*, 2008, 2010; Abo-Naf *et al.*, 2008). Electron-hole pairs and oxygen vacancies generated in the glasses after irradiation play an important role in producing different types of defects and color centers. The RE doped glasses show changes in the valence state of the dopant as well as in its color as a result of photochemical reaction during exposure to gamma irradiation. Zeng *et al.* (2008) reported that Yb^{3+} changes to Yb^{2+} in YAG crystal after gamma irradiation, whereas this process is reversed after annealing of the crystal. A similar change from Nd^{3+} to Nd^{2+} has been reported by Rai *et al.* (1986, 2010, 2012) in neutron irradiated Nd_2O_3 powder and gamma irradiated Nd-doped phosphate glasses. These studies have been carried out using optical spectroscopic techniques, which provide information about the changes in the optical properties such as absorption and photoluminescence in the visible spectral range. The photo-induced coloring of samarium (Sm) and europium (Eu) doped $5\text{Na}_2\text{O}-10\text{Al}_2\text{O}_3-85\text{B}_2\text{O}_3$ glass has been studied by L_3 -edge X-ray absorption near-edge structure (XANES) spectroscopy of Sm and Eu before and after X-ray and UV irradiation. It has been reported that the irradiation effects changed the valence state of the doped ions (Sm and Eu) in the glass matrix (Shimizu-gawa *et al.*, 2001; Rossano *et al.*, 2009). XANES spectra recorded at the L_3 -edge of RE elements are distinguished by a relatively intense absorption peak known as the white line, which occurs due to electronic transition from the $2p$ core level to mainly $5d$ -like states of the RE elements. In the case of low concentration of the RE dopant the XANES spectra provide information about its structural and chemical transformation in a more straightforward way. X-ray photoelectron spectroscopy (XPS) has also proved to be a powerful technique in the study of bulk structural properties of oxide glasses. In particular, this has been used to distinguish between the bridging oxygen (BO) and the non-bridging oxygen

(NBO) atoms in the glasses. Recently, this technique has been used to study the changes in valence state of the ions along with variation in the behavior of the BO and the NBO in laser irradiated phosphate glasses (Khattak *et al.*, 2010, 2013).

The main aim of the present study is to obtain information about the changes in Nd-doped phosphate glasses after gamma irradiation using XANES and XPS techniques. The effect of the ratio of O to Nd on the white line intensity of XANES as well as the variations in the concentration of elements and NBO in the glasses before and after gamma irradiation will also be discussed.

2. Experimental details

2.1. Method of glass preparation

The Nd-doped phosphate glass samples (obtained from CGCRI, Kolkata, India) were prepared using different compositions and combinations of P_2O_5 , K_2O , BaO , Al_2O_3 , AlF_3 , SrO and Nd_2O_3 as base materials (Rai *et al.*, 2011). Different weight percentages of each oxide were used to make four types of glass samples (samples #1 to #4). The melt quenching technique was used to prepare these glasses, where reagents were thoroughly mixed in an agate mortar and placed in a platinum crucible for melting in an electric furnace at 1095°C for 1 h 40 m. The melt was then poured onto a preheated brass plate and annealed at 365°C for 18 h. Finally, the samples were polished to obtain a smooth, transparent and uniform surface slab of thickness 5 mm for different measurements. The elemental compositions of each element (atomic %) in the glasses were measured using energy-dispersive X-ray spectroscopy (EDX) after glass preparation. The spectrum of each sample was recorded before and after gamma irradiation using a Bruker X-Flash SDD EDS detector, 129 eV, in order to obtain the relative concentration of different elements present in the glass samples. Final data were obtained after averaging the data recorded at three random locations in order to compensate for the variation in concentration of elements from one place to another in the same sample. Tables 1 to 3 show the average atomic % of the important elements present in the glass samples before and after gamma irradiation.

2.2. Gamma irradiation of samples

A few small pieces of glass samples were irradiated at room temperature using a ^{60}Co (2490 Ci, Gamma chamber 900) source of gamma radiation having a dose rate of 2 kGy h^{-1} . Samples were irradiated for radiation doses varying from 10 to 500 kGy.

2.3. XANES measurement

Nd L_3 -edge XANES spectra were recorded in fluorescence mode using the energy-scanning EXAFS beamline (BL-9) at Indus-2 synchrotron source (2.5 GeV, 150 mA), Raja Ramanna Centre for Advanced Technology (RRCAT), Indore, India. The beamline optics consist of a Rh/Pt-coated collimating meridional cylindrical mirror followed by a

Si(111)-based double-crystal monochromator (DCM). The second crystal of the DCM is a sagittal cylindrical crystal, which is used for horizontal focusing of the beam, while another Rh/Pt-coated bendable post-mirror facing downwards is used for vertical focusing of the beam at the sample position. An ionization chamber was used to monitor the incident beam flux $I_0(E)$, whereas a Si drift detector (VORTEX-EX) was used to detect the X-ray fluorescence signal $I_f(E)$ from the samples at an angle of 45° with respect to the sample surface, and the absorbance of the sample ($\mu = I_f/I_0$) was obtained as a function of energy by scanning the monochromator over the specified energy range.

X-ray absorption data in the neighborhood of the Nd L_3 -edge (6208 eV) were recorded in the range 6180–6300 eV with a step of 1 eV for all the samples #1 to #4. The XANES spectra of glass sample #3 were recorded before and after gamma irradiation in order to find variation in its properties. The XANES spectrum of commercial Nd_2O_3 was also recorded to calibrate the energy range data obtained from the glass samples. Since Nd L_3 -edge XANES were recorded in fluorescence mode, the XANES data were corrected for self-absorption using the *ATHENA* program (Ravel & Newville, 2005).

2.4. XPS measurement

Core-level photoelectron spectra of the glasses were recorded using Al and Mg K_α radiation ($h\nu = 1486.6$ and 1253.6 eV, respectively) as excitation source during this experiment. O 1s core-level spectra were recorded using a SPECS PHOIBOS 150 electron analyzer whereas other spectra were measured using an OMNICON EA125 electron analyzer. X-ray photoelectron spectra from the Nd $3d$ and O 1s core levels were recorded using a computer-controlled data collection system with the electron analyzer set at a pass energy of ~ 30 eV. The chamber pressure was maintained at $\sim 1.2 \times 10^{-9}$ Torr during this experiment. XPS data were analyzed using *CasaXPS* software. De-convolution curve-fitting was carried out using a non-linear least-squares optimization procedure; Gaussian–Lorentzian (GL50) line shapes were applied with a Shirley background. The C 1s transition at 284.6 eV was used as a reference in order to obtain information about the shift in the spectrum due to accumulation of the space charge (Mekki & Salim, 1999). Normally the C 1s peak occurs due to hydrocarbon contamination, which is supposed to be constant irrespective of the chemical state of the sample. Comparison of the C 1s spectra showed negligible shift in the peaks.

In this experiment, XPS results have been used to obtain qualitative information about the glass structure as well as to support the results obtained from the XANES measurements.

3. Results and discussion

3.1. X-ray absorption spectroscopy (XANES) of glasses

Nd L_3 -edge XANES spectra corresponding to samples #1 to #4 of Nd-doped phosphate glasses are shown in Fig. 1 along

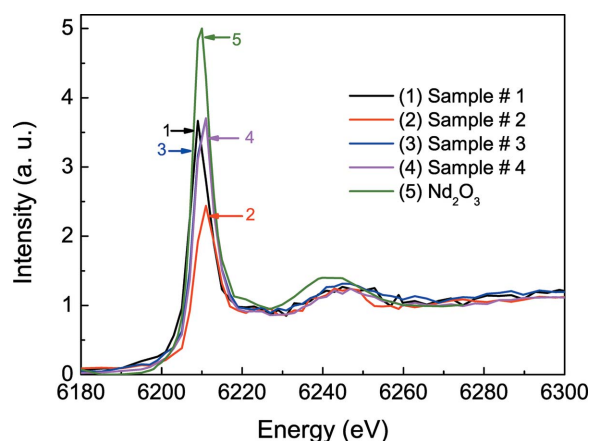


Figure 1
Nd L_3 -edge XANES spectra of Nd_2O_3 and Nd-doped phosphate glasses. (1) Sample #1, (2) Sample #2, (3) Sample #3, (4) Sample #4 and (5) Nd_2O_3 .

with that of a commercial Nd_2O_3 sample. The L_3 -edge energy was ~ 6208 eV for all the glass samples, which is in close agreement with results reported in the literature. This shows that the spectroscopic valence state of Nd in the glass samples is maintained regardless of the local structural arrangement resulting from changes in the composition of glasses. All the samples show a white line peak, which arises due to the $2p \rightarrow 5d$ ($^2P_{3/2} \rightarrow ^2D_{5/2}$) transition (Rao *et al.*, 1983). The presence of similar white line peaks indicates the identical spectroscopic nature of Nd in the glass samples. The small peak at ~ 6240 eV after the white line peak is due to multiple electron scattering contributions. The white line peaks due to samples #1 and #3 are observed at 6209 eV whereas for samples #2 and #4 they appear at 6211 eV. The peak intensities of samples #1, #3 and #4 are nearly the same but found to be smaller in the case of sample #2. This indicates that the edge and the peak energy of the white lines are slightly affected by local structural modifications (changes in the neighboring atoms) in the glasses, which occur due to small changes in the composition of the glasses. Fig. 1 further shows that the XANES spectra of Nd doped in the phosphate glasses and in crystalline Nd_2O_3 are quite similar. This suggests that the local environment of Nd^{3+} in both cases is very similar. Even the coordination geometry around Nd^{3+} in the glass and in the oxide seem to be similar. Normally, the XANES spectra arising from the same absorbing atom in different coordination geometries are expected to be different. However, observation of a close similarity in the XANES spectral features of Nd_2O_3 and $\text{NdF}_3\text{-BeF}_2$ glass was also reported earlier (Rao *et al.*, 1983).

Small changes in the position and the intensity of the white line peaks among the glass samples are found to be correlated with the concentration of Nd as well as with the ratio of the oxygen and the Nd atoms (O/Nd), because oxygen atoms are supposed to be present around Nd^{3+} in the oxide glass matrix. Table 1 shows that samples #1 and #3 have a quite similar concentration of Nd in the glass matrix, ~ 0.32 and $\sim 0.28\%$, whereas samples #2 and #4 have concentrations of ~ 0.09 and $\sim 0.19\%$, respectively. This indicates that the lowest concentration of Nd in sample #2 is contributing to the small

Table 1

Elemental composition (atomic %) and O/Nd ratio present in the glass samples (EDX data).

| Sample number | Atomic component | Sample #1 (at%) | Sample #2 (at%) | Sample #3 (at%) | Sample #4 (at%) |
|---------------|------------------|-----------------|-----------------|-----------------|-----------------|
| 1 | O | 77.84 ± 6.35 | 82.32 ± 5.50 | 81.06 ± 5.60 | 77.87 ± 7.47 |
| 2 | P | 13.20 ± 0.60 | 10.27 ± 0.43 | 9.99 ± 0.43 | 13.64 ± 0.73 |
| 3 | Ba | 1.94 ± 0.45 | 1.32 ± 0.26 | 1.77 ± 0.37 | |
| 4 | K | 3.96 ± 0.25 | 3.58 ± 0.16 | 4.73 ± 0.20 | 3.19 ± 0.20 |
| 5 | Al | 2.27 ± 0.10 | 2.00 ± 0.13 | 1.97 ± 0.10 | 3.99 ± 0.30 |
| 6 | Nd | 0.32 ± 0.13 | 0.09 ± 0.10 | 0.28 ± 0.10 | 0.19 ± 0.10 |
| 7 | O/Nd | 243.25 | 914.67 | 289.5 | 409.84 |

amplitude of the white line peak of the XANES spectra. In other words, the white line intensity is found to be lowest where the ratio O/Nd (~ 914.66) is highest in the glass samples. The small shift in the white line peak towards higher energy also seems to be related to the comparatively higher value of the O/Nd ratio in samples #2 and #4, *i.e.* 914.66 and 409.84 in comparison with 243.25 and 289.50 for samples #1 and #3, respectively. This shows that a higher value of the O/Nd ratio affects the electric field around Nd in the glass matrix, which ultimately affects the energy level of the final $^2D_{5/2}$ state of Nd^{3+} and consequently generates a slight change in the peak position of the white line. These observations are due to the change in the covalence of the RE–O chemical bond in the glass matrix. It has been reported that the local atomic environments surrounding the RE atoms as well as the covalence character of the RE chemical bonds play an important role in the optical emission from RE doped glasses (Choi, 2006; Choi *et al.*, 2007). In fact, the covalence of the RE–O chemical bond, the ratio O/Nd and the coordination number are correlated with changes in the structural properties of the glass. However, the white line intensity cannot be described only in terms of the covalence of the chemical bonds formed by RE elements. It has been reported that a close connection exists between the X-ray absorption $\mu = \mu_0(1 + \chi)$ and the electronic structure, *i.e.* the local electronic density of states $\rho = \rho_0(1 + \chi)$ (Ankudinov *et al.*, 1998), where μ_0 and ρ_0 both represent the atomic background contributions and the oscillating function χ determines the fine structure. Normally, when the covalence of RE bonds is enhanced, the transition probability of the $2p \rightarrow 5d$ transition also increases due to the screening effect. Sometimes it decreases in some of the glasses (Choi, 2006). This indicates that a careful evaluation is needed regarding the factors affecting the XANES spectra such as the screening effect on the electronic transition along with differences in the multiple scattering and the local density of states, which require further investigation.

3.2. Effect of gamma irradiation on XANES of glasses

Fig. 2 shows the L_3 -edge XANES spectra of Nd present in Nd_2O_3 as well as in glass sample #3 before and after gamma irradiation (10 and 100 kGy), which shows that the white line peak intensity of sample #3 decreases after gamma irradiation (10 kGy). The peak intensity decreases further with an increase in the gamma irradiation dose from 10 kGy to 100 kGy. The decrease in the L_3 -edge peak intensity of the

white line of Nd in gamma-irradiated Nd-doped glass samples seems to be due to a change in the elemental concentration surrounding the Nd atom as a result of bond breaking. However, the change in the concentrations of oxygen and Nd are very small in sample #3 in comparison with that in sample #1 after gamma irradiation as can be seen from the EDX measurements (Tables 2 and 3).

Any change in the oxidation state of the REs after irradiation can affect the white line peak intensity. A decrease in the white line intensity from XANES of Sm^{3+} and Eu^{3+} has been reported after X-ray irradiation of Sm- and Eu-doped $Na_2O-Al_2O_3-B_2O_3$ glass samples (Shimizugawa *et al.*, 2001). Sm^{3+} and Eu^{3+} ions in glass samples were found to be reduced to Sm^{2+} and Eu^{2+} after X-ray irradiation. In addition, the pre-edge peak intensity in the XANES spectra of glasses due to Sm^{2+} and Eu^{2+} increased with an increase in the doses of X-ray irradiation. This clearly indicates that the number density of Sm^{3+} and Eu^{3+} decreases whereas the corresponding number density of Sm^{2+} and Eu^{2+} increases in the glass sample as a result of X-ray irradiation. In fact, the presence of these pre-edge peaks in the spectra recorded from the un-irradiated glass samples indicated the existence of both types of oxidation state (as 3+ and 2+) for Sm and Eu in the $Na_2O-Al_2O_3-B_2O_3$ glass samples. In another experiment, Rossano *et al.* (2009) reported a similar variation in the white line intensity of XANES spectra of an iron-bearing soda lime glass system after beta irradiation and concluded that Fe^{3+} was reduced to Fe^{2+} during the irradiation process.

Thus, the change in the white line peak intensity in the case of the present sample can be due to the change in the oxidation state of Nd from Nd^{3+} to Nd^{2+} after gamma irradiation. However, experimentally no chemical shift or change in the absorption-edge spectra (the spectral profile of the white line) is observed as a result of a change in the oxidation state of

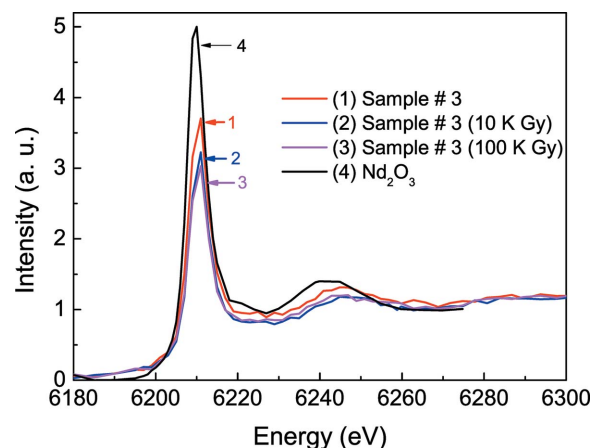


Figure 2

Nd L_3 -edge XANES spectra of Nd_2O_3 and Nd-doped glass before and after gamma irradiation. (1) Sample #3, (2) sample #3 irradiated at 10 kGy, (3) sample #3 irradiated at 100 kGy, (4) Nd_2O_3 .

Table 2

Elemental composition (atomic %) and O/Nd ratio present in sample #1 before and after gamma irradiation (EDX data).

| Atomic composition | O | P | Ba | K | Al | Nd | O/Nd |
|--|--------------|--------------|-------------|-------------|-------------|-------------|--------|
| Average atomic % | 77.84 ± 6.35 | 13.20 ± 0.60 | 1.94 ± 0.45 | 3.96 ± 0.25 | 2.27 ± 0.10 | 0.32 ± 0.13 | 243.25 |
| Average atomic % (γ irradiated 10 kGy) | 75.45 ± 4.40 | 12.86 ± 0.50 | 2.38 ± 0.30 | 5.27 ± 0.2 | 3.08 ± 0.10 | 0.30 ± 0.10 | 251.50 |
| Average atomic weight % (γ irradiated 500 kGy) | 66.19 ± 4.3 | 17.00 ± 0.60 | 3.12 ± 0.45 | 5.90 ± 0.25 | 3.99 ± 0.15 | 0.37 ± 0.10 | 178.89 |

Nd³⁺ to Nd²⁺ in this sample. This is either due to no change in the oxidation state of Nd after irradiation or due to a fast recovery of the converted (induced) Nd²⁺ into Nd³⁺ in a few days after irradiation as has been reported earlier in the case of neutron-irradiated Nd₂O₃ powder (Rai *et al.*, 1986). It is important to mention here that Nd has only one stable oxidation state, Nd³⁺. Here the second possibility seems to be more probable, because the XANES experiment was performed a few months after irradiation.

3.3. XPS of phosphate glasses

3.3.1. Nd 3d spectra. X-ray photoelectron spectra of Nd-doped phosphate glasses (#1 and #3) were recorded before and after gamma irradiation using an Al K α X-ray source. In this section, attention is paid mainly to the core-level spectrum of Nd 3d in order to study the effect of gamma irradiation. Fig. 3 shows the XPS spectra of glass sample #1 before and after 10 and 500 kGy gamma irradiation. The fresh sample shows two broad peaks at ~982.5 and ~1003.7 eV due to 3d_{5/2} and 3d_{3/2} (Nd 3d spectra). It is observed that these peaks become sharper in the case of gamma-irradiated samples, accompanied by a shift to higher binding energies. This observation of sharpening and shift in the Nd 3d peaks is found due to a decrease in the oxygen content in the glass samples after gamma irradiation. Normally some of the oxygen peaks and Nd 3d peaks are very closely spaced and merge together forming a combined broad peak in the case of a fresh sample, which sharpens due to the loss of oxygen from the glass samples after gamma irradiation. This is in agreement

with data obtained from EDX, which show a decrease in the elemental concentration of the oxygen in glass sample #1 after gamma irradiation (Table 2). A drastic decrease in the concentration of oxygen in glass sample #1 is noted in the case of heavy irradiation dose (500 kGy). However, the decrease in the concentration of oxygen in the EDX data is very low/negligible for low doses of gamma irradiation (10 kGy). In spite of this, both samples #1 and #3 show a sharp Nd 3d peak due to 3d_{5/2} after a low dose of gamma irradiation (10 kGy) (Fig. 4). It can also be noted that the main peak of sample #3 shifts to lower energy and is broad in comparison with the peak due to sample #1, which is due to the presence of AlF₃ and a higher concentration of oxygen in the sample #3 network. Further, the intensity of the Nd 3d_{5/2} peak shows a decreasing trend after gamma irradiation (Fig. 3). The intensity of this peak is comparatively higher in the case of a gamma irradiation dose of 500 kGy than for 10 kGy. Such changes in the intensity of peaks are due to the relative change in the concentration of elements after gamma irradiation that is possible as a result of bond breaking, and its reorganization in the glass samples under the effect of gamma irradiation was reported earlier during Fourier transform infrared (FTIR) studies of these glasses (Rai *et al.*, 2011). However, variation in the elemental concentration in the glass sample is also possible as a result of diffusion of ions from surface to bulk and *vice versa* along with the emission of oxygen after gamma irradiation. Here the possibility of a change in the concentration of Nd due to the change in the oxidation state from Nd³⁺ to Nd²⁺ is ruled out because such changes are not stable and recovery is very fast, *i.e.* a few days as has been reported earlier (Rai *et al.*, 1986). The effect of gamma irradiation has also been observed in the form of darkening the color of Nd-

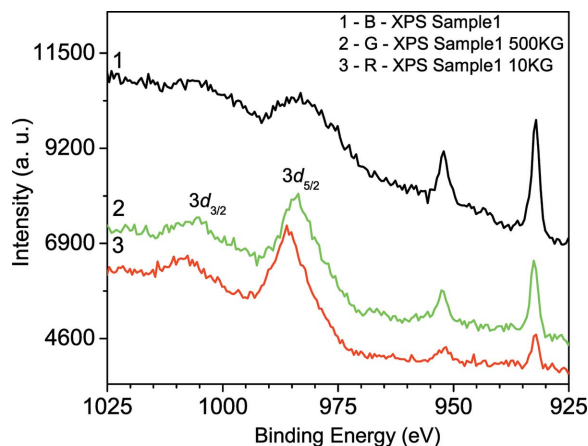


Figure 3 XPS spectra of Nd 3d from sample #1 before and after gamma irradiation. (1) Pure sample #1, (2) sample #1 irradiated at 500 kGy, (3) sample #1 irradiated at 10 kGy (using Al K α source $h\nu = 1486.6$ eV).

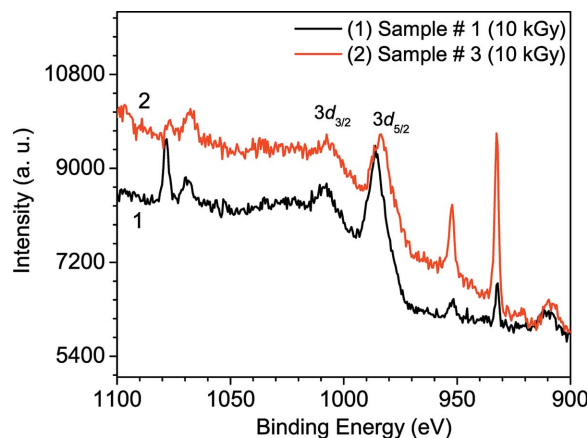


Figure 4 XPS spectra of Nd 3d from glass samples after gamma irradiation of 10 kGy. (1) Sample #1, (2) sample #3 (using Al K α source $h\nu = 1486.6$ eV).

Table 3

Elemental composition (atomic %) and O/Nd ratio present in sample #3 before and after gamma irradiation (EDX data).

| Atomic component | O | P | Ba | K | Al | Nd | O/Nd |
|--|--------------|-------------|-------------|-------------|-------------|-------------|--------|
| Average atomic % | 81.06 ± 5.60 | 9.99 ± 0.43 | 1.77 ± 0.37 | 4.73 ± 0.20 | 1.97 ± 0.10 | 0.28 ± 0.10 | 289.5 |
| Average atomic % (γ irradiated 10 kGy) | 82.83 ± 8.40 | 7.21 ± 0.40 | 0.49 ± 0.20 | 0.99 ± 0.10 | 3.85 ± 0.25 | 0.34 ± 0.15 | 243.62 |

doped phosphate glasses. Similar darkening in the glass sample has been reported in the case of X-ray irradiated Sm- and Eu-doped $\text{Na}_2\text{O}-\text{Al}_2\text{O}_3-\text{B}_2\text{O}_3$ glasses (Shimizugawa *et al.*, 2001). These observations are due to the generation of different types of photo-induced defects in the glasses including oxygen vacancies.

As discussed in the previous section, the XPS and EDX measurements indicate that the concentration of oxygen in the glass samples decreases after gamma irradiation. Similar variations in XPS of Nd containing alloy glass have also been reported by Tanaka *et al.* (1994). They found that the presence of a higher concentration of oxygen in the glass induces broadening in the $3d_{5/2}$ and $3d_{3/2}$ peaks due to Auger O *KLL* and $3d$ satellite peaks. An O *KLL* peak represents the energy of the electrons ejected from the atoms due to filling of the O $1s$ state (*K* shell) by an electron from the *L* shell coupled with the ejection of an electron from the *L* shell. Such broadening in Nd ($3d$) peaks due to the presence of extra peaks from oxygen is not observed in the samples where the oxygen content is less. The decrease in oxygen content is accompanied by a small shift of the main peak (Nd $3d$) towards higher energy. In order to verify that the broadening in the Nd $3d$ peaks is due to overlapping of the O *KLL* peak of oxygen, the XPS spectra (O *KLL*) of sample #1 were recorded using a Mg K_α source before and after gamma irradiation (Fig. 5). It is noted that O *KLL* spectra are observed near ~ 750 eV whereas Nd $3d$ peaks (not shown in Fig. 5) are observed at the same location as that observed using the Al K_α source. This is as expected because the binding energies in

XPS are fixed whereas the Auger kinetic energies are fixed. In this situation the change in X-ray source changes the location of the O *KLL* peak while keeping the Nd $3d$ peaks at the same location. It is also observed that the profiles of the Nd $3d$ peaks recorded before and after gamma irradiation are almost similar whereas the area of the O *KLL* peaks decreases after gamma irradiation (inset of Fig. 5). This clearly indicates that the sharpening of the broad Nd $3d$ peaks after gamma irradiation, as observed in the case of the Al K_α source (Fig. 3), is due to oxygen deficiency in the glass sample that induces sharpening in the O *KLL* peak. A similar decrease in oxygen concentration has been reported by Puglisi *et al.* (1983) after electron beam irradiation of glass samples. They used XPS to study the compositional changes in the glass samples after electron beam irradiation and reported an out-gassing of oxygen from the sample. A similar observation was noted in the EDX measurement data (Tables 2 and 3) in the present experiment, which shows that each and every element present in the glass samples shows some variation in their relative concentration after gamma irradiation. Normally both XPS and EDX are effective mainly on the surfaces as X-rays cannot penetrate the glass samples. Therefore, it cannot provide information about the elements present in the bulk sample. As per the above discussion the decrease in the width of the XPS Nd $3d_{5/2}$ peak also seems to be associated with a decrease in the O/Nd ratio in the glass after gamma irradiation, where diffusion of the elements from the surface to inside the bulk material may be playing an important role. A similar observation has been reported by Khattak *et al.* (2013) regarding the decrease in concentration of vanadium in vanadium phosphate glass after laser irradiation, which is supposed to be either due to evaporation of vanadium from the surface of the glass or due to its diffusion from the surface to the bulk. This indicates that high-energy irradiation changes the relative concentration of the elements along with out-gassing of the oxygen from the glass samples.

3.3.2. O $1s$ spectra. XPS study of oxide glasses provides O $1s$ spectra that have proved to be more informative with respect to the structure of the glasses. The binding energy of the O $1s$ electrons is a measure of the extent to which electrons are localized on the oxygen or in the inner-nuclear region. This is a direct consequence of the nature of the bonding between the oxygen and the other cations present in the glass samples (Khattak *et al.*, 2010, 2013). The XPS O $1s$ spectra for sample #1 before and after gamma irradiation (10 and 500 kGy) are shown in Fig. 6. A slight asymmetry is observed in the profile of the O $1s$ peak obtained from fresh glass sample #1 (Fig. 6), which indicates the presence of two different types of oxygen sites in this glass. This asymmetry is observed towards the higher energy side. A similar asymmetry

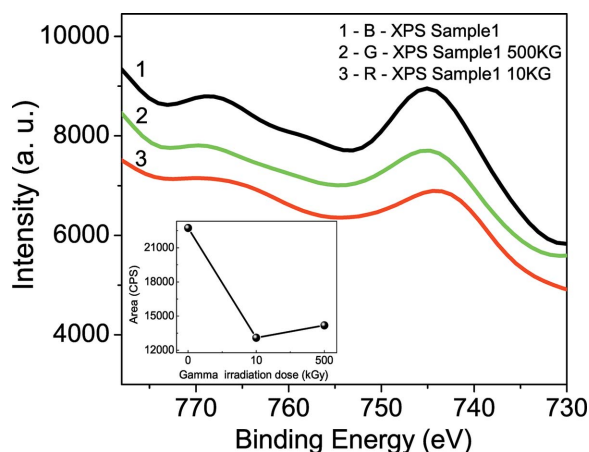


Figure 5

XPS spectra of O *KLL* from sample #1 before and after gamma irradiation. (1) Pure sample #1, (2) sample #1 irradiated at 500 kGy, (3) sample #1 irradiated at 10 kGy (using Mg K_α source $h\nu = 1254.6$ eV). The inset shows variation of O *KLL* peak area as a function of gamma irradiation dose.

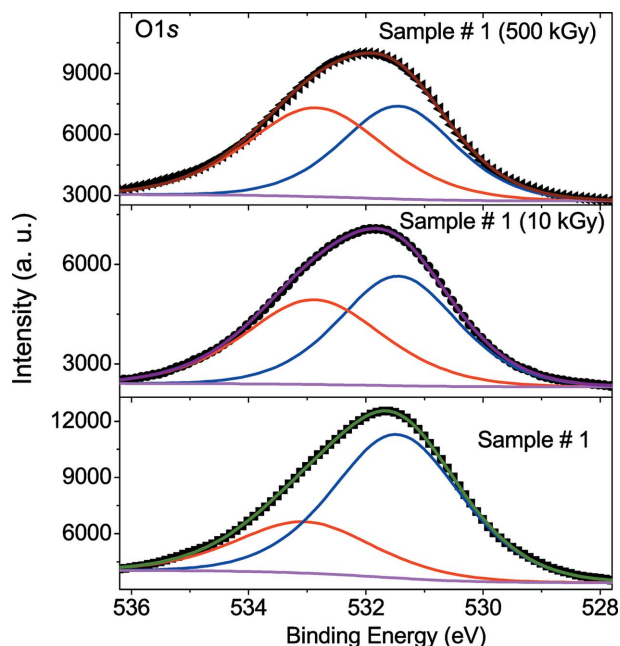


Figure 6
XPS spectra of the oxygen O 1s core level. (1) Sample #1, (2) sample #1 irradiated at 10 kGy, (3) sample #1 irradiated at 500 kGy. Scatter represents experimental data whereas solid lines are best fitting (using Al K_{α} source $h\nu = 1486.6$ eV). The fitted high-energy peak is due to BO and the low-energy peak is due to NBO.

in O 1s spectra has been reported in different types of glasses by many researchers (Khattak *et al.*, 2010, 2013; Mekki *et al.*, 1996). Normally, an asymmetry in the O 1s core-level peaks occurs due to the presence of two different types of oxygen sites in the glasses. The O 1s peaks for these phosphate glasses may arise from oxygen atoms existing in some or all of the following structural bonds: P–O–P, P–O–Nd, Nd–O–Nd, P=O and P–O–M, where M represents other cations present in the glass matrix. The oxygen atoms that have covalent bonding with the glass-former atoms on both the sides are typically called BO such as P–O–P, whereas the oxygen atoms that are more ionically bonded at least on one side or double bonded to glass-former atoms are referred to as NBO such as P–O–Nd, Nd–O–Nd, P=O (Khattak *et al.*, 2010). In this situation the binding energy of NBO remains lower than that of BO. This profile becomes nearly symmetric after gamma irradiation (10 and 500 kGy) probably due to a change in the number density of BO and NBO as a result of either bond breaking or reorganization of the bonds. A similar asymmetry has been noted in the case of the O 1s spectrum from sample #3 as shown in Fig. 7, which also changes after gamma irradiation. The O 1s spectrum is fitted by two Gaussian–Lorentzian peaks in order to determine the peak position and the relative contribution of the different oxygen sites in the glasses. The data obtained from this fitting are shown in Table 4. This shows that the ratio of NBO to total oxygen decreases in the case of sample #1, whereas it increases in the case of sample #3, with an increase in the doses of gamma irradiation. It seems that the reorganization process of the bonds plays an important role in the case of sample #1 in comparison with sample #3. An increase in the ratio of NBO

Table 4
Peak position and total area of O 1s after XPS peak fitting of O 1s core-level spectra.

| Sample | O 1s peak position (eV) | | | Total area |
|---------------------|-------------------------|--------|------------------------|------------|
| | NBO | BO | NBO/O _{total} | |
| Sample #1 | 531.51 | 533.09 | 0.72373 | 30283.6 |
| Sample #1 (10 kGy) | 531.45 | 532.91 | 0.52841 | 16617.6 |
| Sample #1 (500 kGy) | 531.45 | 532.85 | 0.46447 | 24958 |
| Sample #3 | 531.33 | 532.78 | 0.42398 | 27725.3 |
| Sample #3 (10 kGy) | 531.35 | 532.71 | 0.43607 | 27515.4 |
| Sample #3 (100 kGy) | 531.34 | 533.2 | 0.7732 | 42457.6 |

to total oxygen in sample #3 with an increase in the gamma irradiation indicates that the number of defects increases in this sample. The other defects such as oxygen vacancies as well as trapped electron and hole centers will also increase with an increase in the gamma irradiation dose. The presence of different types of defects in these glasses has been studied optically and is found to be in agreement with the present results (Rai *et al.*, 2010). The generation of comparatively more defects in sample #3 after gamma irradiation proves this glass as soft material for gamma irradiation. In other words, sample #1 is more radiation resistant than sample #3. Finally, these observations are in line with results obtained from optical and FTIR spectra of these samples indicating that gamma irradiation increases the breaking of P–O–P linkages and creating NBO in the form of P=O, P–O–Nd and/or P–O–M linkages (Rai *et al.*, 2011). However, dominant reorganization of bonds has also been noted in sample #1 after gamma irradiation in the form of a decrease in the concentration of NBO (Table 4). The composition of glass

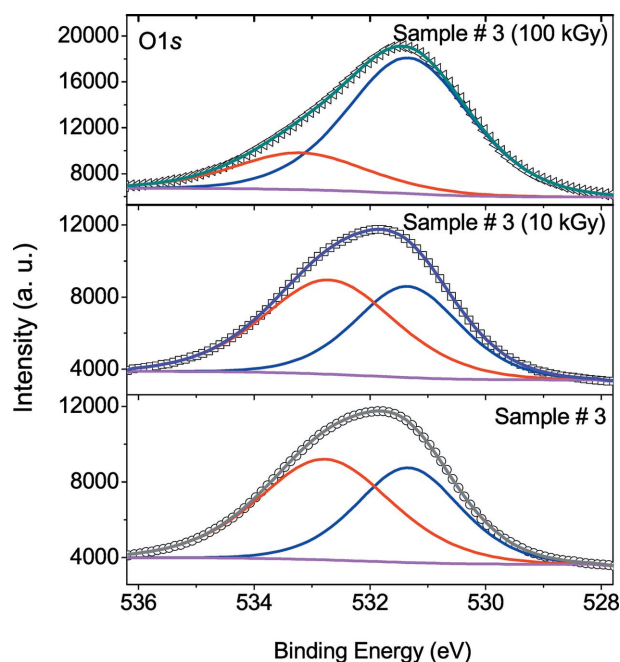


Figure 7
XPS spectra of the oxygen O 1s core level. (1) Sample #3, (2) sample #3 irradiated at 10 kGy. Scatter represents experimental data whereas solid lines are best fitting (using Al K_{α} source $h\nu = 1486.6$ eV). The fitted high-energy peak is due to BO and the low-energy peak is due to NBO.

samples #1 and #3 shows that sample #3 has a higher percentage of oxygen, whereas the other elemental compositions are nearly similar. This indicates that more oxygen in sample #3 makes this glass comparatively soft for gamma irradiation.

4. Conclusions

The observation of a similarity in the XANES spectra of Nd-doped phosphate glass and Nd_2O_3 suggests that both structures may have a similar coordination geometry around Nd^{3+} . The white line peak intensity due to L_3 -edge XANES of Nd and its location are found to be mainly dependent on the variation in the concentration of elements present around Nd as well as on the ratio O/Nd in the glass samples. In particular, the decrease in the white line peak intensity of Nd XANES in the glasses after gamma irradiation seems to be due to a change in the covalence of the chemical bonds in the glass samples. Variation in the elemental concentration in the glass samples after gamma irradiation as measured by EDX may be due to diffusion of elements from surface to bulk and *vice versa* in the glasses. The sharpening of the Nd $3d_{5/2}$ peak (XPS) after gamma irradiation indicates the deficiency of oxygen atoms in the glass matrix. Comparison of the O 1s spectra of glass samples #1 and #3 recorded before and after gamma irradiation shows that the ratio of NBO to total oxygen decreases in sample #1 whereas it increases in sample #3 after gamma irradiation. This indicates dominant reorganization of the bonds in sample #1. The presence of a large number of NBO in sample #3 after gamma irradiation indicates the presence of a comparatively large number of defects in this glass. This makes sample #1 more radiation resistant than sample #3. It seems that the oxygen-rich glass samples are comparatively soft to gamma irradiation. Finally, the above results along with optical observations (Rai *et al.*, 2010) indicate that the generation of different types of defects such as oxygen vacancies, trapped electron and hole centers after gamma irradiation seems to be the reason for glass coloration in the present experiment.

Acknowledgements

M. P. Kamat, HPLOL, RRCAT, Indore, is thankfully acknowledged for providing glass samples for this study. The authors are grateful to S. Kher, Pragya Tiwari, D. M. Phase and A. Wadikar for providing various experimental help and discussions during this work. We also thank P. A. Naik and N. K. Sahoo for their keen interest and encouragement during this work.

References

Abo-Naf, S. M., El-Amiry, M. S. & Abdel-Khalek, A. A. (2008). *Opt. Mater.* **30**, 900–909.
 Ajith Kumar, G., Biju, P. R., Venugopal, C. & Unnikrishnan, N. V. (1997). *J. Non-Cryst. Solids*, **221**, 47–58.
 Ajroud, M., Haouari, M., Ouada, H., Maaref, H., Brenier, A. & Garapon, C. (2000). *J. Phys. Condens. Matter*, **12**, 3181–3193.

Ankudinov, A. L., Ravel, B., Rehr, J. J. & Conradson, S. D. (1998). *Phys. Rev. B* **58**, 7565.
 Balakrishnaiah, R., Babu, P., Jayasankar, C. K., Joshi, A. S., Speghini, A. & Bettinelli, M. (2006). *J. Phys. Condens. Matter*, **18**, 165–179.
 Beber, M. J. (1986). Editor. *Handbook of Laser Science and Technology*, Vol. III–V. Boca Raton: CRC Press.
 Campbell, J. H. & Suratwala, T. I. (2000). *J. Non-Cryst. Solids*, **263–264**, 318–341.
 Choi, Y. G. (2006). *Met. Mater. Intl*, **15**, 993–999.
 Choi, Y. G., Lee, K. A. & Lee, K. S. (2007). *Met. Mater. Int.* **13**, 269–273.
 Day, D. E., Wu, Z., Ray, C. S. & Hrma, P. (1998). *J. Non-Cryst. Solids*, **241**, 1–12.
 Dwivedi, Y. & Rai, S. B. (2012). *Appl. Phys. A*, **109**, 213–218.
 Ebendorff-Heidepriem, H., Seeber, W. & Ehrhart, D. (1995). *J. Non-Cryst. Solids*, **183**, 191–200.
 ElBatal, F. H. (2007). *Nucl. Instrum. Methods Phys. Res. B*, **265**, 521.
 ElBatal, F. H., Hamdy, Y. M. & Marzouk, S. Y. (2008). *Mater. Chem. Phys.* **112**, 991–1000.
 ElBatal, F. H., Ouis, M. A., Morsi, R. M. M. & Marzouk, S. Y. (2010). *J. Non-Cryst. Solids*, **356**, 46–55.
 Friebele, E. J. (1991). *Radiation Effects on Optical Properties of Glass*, edited by D. R. Uhlmann and N. J. Kreidl, pp. 205–260. Westerville: American Ceramic Society.
 Gatterer, K., Pucker, G., Jantscher, W., Fritzer, H. P. & Arafa, S. (1998). *J. Non-Cryst. Solids*, **231**, 189–199.
 Hussin, R., Holland, D. & Dupree, R. (2002). *J. Non-Cryst. Solids*, **298**, 32–42.
 Jamnický, M., Znášik, P., Tunega, D. & Ingram, M. D. (1995). *J. Non-Cryst. Solids*, **185**, 151–158.
 Jayasankar, C. K., Balakrishnaiah, R., Venkatramu, V., Joshi, A. S., Speghini, A. & Bettinelli, M. (2008). *J. Alloys Compd.* **451**, 697–701.
 Karabulut, M., Marasinghe, G. K., Ray, C. S., Day, D. E., Waddill, G. D., Booth, C. H., Allen, P. G., Bucher, J. J., Caulder, D. L. & Shuh, D. K. (2002). *J. Non-Cryst. Solids*, **306**, 182–192.
 Karthikeyan, B. & Mohan, S. (2004). *Mater. Res. Bull.* **39**, 1507–1515.
 Khattak, G. D., Mekki, A. & Gondal, M. A. (2010). *Appl. Surf. Sci.* **256**, 3630–3635.
 Khattak, G. D., Mekki, A. & Gondal, M. A. (2013). *J. Phys. Chem. Solids*, **74**, 13–17.
 Kumar, A., Rai, D. K. & Rai, S. B. (2003). *Spectrochim. Acta A*, **59**, 917–925.
 Mekki, A., Holland, D., McConville, C. F. & Salim, M. (1996). *J. Non-Cryst. Solids*, **208**, 267–276.
 Mekki, A. & Salim, M. (1999). *J. Electron Spectrosc. Relat. Phenom.* **101–103**, 227–232.
 Metwalli, E., Karabulut, M., Sidebottom, D. L., Morsi, M. M. & Brow, R. K. (2004). *J. Non-Cryst. Solids*, **344**, 128–134.
 Minami, T., Imazawa, K. & Tanaka, M. (1980). *J. Non-Cryst. Solids*, **42**, 469–476.
 Pérez-Rodríguez, C., Martín, L. L., León-Luis, S. F., Martín, I. R., Kumar, K. & Jayasankar, C. K. (2014). *Sens. Actuators B*, **195**, 324–331.
 Puglisi, O., Marletta, G. & Torrisi, A. (1983). *J. Non-Cryst. Solids*, **55**, 433–442.
 Rai, V. N., Raja Sekhar, B. N. & Jagtap, B. N. (2012). *Asia. J. Spectrosc. Special Issue* 121.
 Rai, V. N., Raja Sekhar, B. N., Kher, S. & Deb, S. K. (2010). *J. Lumin.* **130**, 582–586.
 Rai, V. N., Sekhar, B. N. R., Tiwari, P., Kshirsagar, R. J. & Deb, S. K. (2011). *J. Non-Cryst. Solids*, **357**, 3757–3764.
 Rai, V. N., Thakur, S. N. & Rai, D. K. (1986). *Appl. Spectrosc.* **40**, 1211–1214.
 Rao, K. J., Wong, J. & Weber, M. J. (1983). *J. Chem. Phys.* **78**, 6228.
 Ravel, B. & Newville, M. (2005). *J. Synchrotron Rad.* **12**, 537–541.

- Rossano, S., Jean-Soro, L., Boizot, B., Farges, F., van Hullebusch, E., Labanowski, J., Gouzin, L., Combes, R., Linares, J., Swarbrick, J. C. & Harfouche, M. (2009). *J. Phys. Conf. Ser.* **190**, 012194.
- Sandhu, A. K., Singh, S. & Pandey, O. P. (2008). *J. Phys. D*, **41**, 165402.
- Satyanarayana, N., Govindaraj, G. & Karthikeyan, A. (1991). *J. Non-Cryst. Solids*, **136**, 219–226.
- Seshadri, M., Venkata Rao, K., Lakshmana Rao, J., Koteswara Rao, K. S. R. & Ratnakaram, Y. C. (2010). *J. Lumin.* **130**, 536–543.
- Sharma, G., Singh, K., Manupriya, Mohan, S., Singh, H. & Bindra, S. (2006). *Radiat. Phys. Chem.* **75**, 959–966.
- Shimizugawa, Y., Umesaki, N., Hanada, K., Sakai, I. & Qiu, J. (2001). *J. Synchrotron Rad.* **8**, 797–799.
- Sudhakar, K. V. S., Srinivasa Reddy, M., Srinivasa Rao, L. & Veeraiah, N. (2008). *J. Lumin.* **128**, 1791–1798.
- Sun, D., Luo, J., Zhang, Q., Xiao, J., Xu, J., Jiang, H. & Yin, S. (2008). *J. Lumin.* **128**, 1886–1889.
- Tanaka, K., Yamada, M., Okamoto, T., Narita, Y. & Takaki, H. (1994). *Mater. Sci. Eng. A*, **181–182**, 932–936.
- Weber, M. J. (1990). *J. Non-Cryst. Solids*, **123**, 208–222.
- Zeng, X., Xu, X., Wang, X., Zhao, Z., Zhao, G. & Xu, J. (2008). *Spectrochim. Acta A*, **69**, 860–864.